Yield correlations and p_T dependence of charmed hadrons in Pb + Pb collisions at $\sqrt{s_{NN}} = 2.76$ TeV

Rui-qin Wang,[1,2] Jun Song,[3] and Feng-lan Shao[1,*]
[1]*Department of Physics, Qufu Normal University, Shandong 273165, China*
[2]*School of Physics, Shandong University, Jinan, Shandong 250100, China*
[3]*Department of Physics, Jining University, Shandong 273155, China*
(Received 19 November 2013; revised manuscript received 11 December 2014; published 30 January 2015)

Recently the ALICE Collaboration has published a few data of charm hadrons in Pb + Pb collisions at the CERN Large Hadron Collider (LHC). We extend the quark combination to the charm sector to deduce the yield formulas of charm hadrons and point out that the measurement of charm hadron yields can provide important insights into charm quark hadronization mechanism in high energy reactions. We propose several types of yield ratios, e.g., D^{*+}/D^0, D_s^+/D^+, and Λ_c^+/D_s^+, to measure various properties of low p_T charm quark hadronization. We argue that ratios D_s^+/D^0 and $2D_s^+/(D^0 + D^+)$ as the function of transverse momentum (p_T) can serve as good probes for the dynamics of charm quark hadronization. We further make predictions for the yields and p_T spectra of identified charm hadrons in central Pb + Pb collisions at $\sqrt{s_{NN}} = 2.76$ TeV.

DOI: 10.1103/PhysRevC.91.014909 PACS number(s): 25.75.Ag, 25.75.Dw, 25.75.Gz

I. INTRODUCTION

Collisions of heavy nuclei with ultrarelativistic collision energies provide conditions for the creation of a new phase quark gluon plasma (QGP) in the laboratory. Hadrons containing charm quarks are powerful tools to study this high density and strong interacting QGP [1–4]. Measurements on charm hadrons have been executed at the BNL Relativistic Heavy Ion Collider (RHIC) [5,6] and recently at the CERN Large Hadron Collider (LHC) [7–10]. With the increase of collision energy from RHIC to LHC, the production of charm quarks increases rapidly. At LHC energies, charm quarks produced in QGP stage become comparable to those produced in initial hard rescatterings [11–13]. In addition, re-interactions of charm quarks with partons in QGP are also enhanced with collision energy from the increasing temperature and energy density of the medium produced in collisions [11–14]. The hadronization of charm quarks is an important topic in charm field because it plays a role of translating these initial or early effects into hadronic observables, and has attracted lots of attentions [15–20]. Quark combination mechanism (QCM) is one of the effective phenomenological methods to describe charm quark hadronization. It has shown its success early in studying flavor dependencies of open charm meson and baryon production in elementary hadronic collisions [21–25] and has many applications in heavy ion collisions recently [15–18].

In this paper, we extend the quark combination model in Refs. [26,27] by including charm quarks to study the yield correlations and p_T dependence of charm hadrons in central Pb + Pb collisions at $\sqrt{s_{NN}} = 2.76$ TeV. Such systematic investigation can provide a better test for the quark combination mechanism and further understanding of the dynamics of hadron production at hadronization. Hadron yield correlations, measured mainly by the ratios of yields of different hadrons, are one kind of effective probes for the mechanism of hadron production in high energy reactions [26,28–32]. We study several kinds of two-particle yield ratios such as D^{*+}/D^0, D_s^+/D^+, and Λ_c^+/D_s^+ as well as multiparticle yield correlations, by virtue of which we explore the properties of low p_T charm quark hadronization from different aspects. Furthermore, we study p_T spectra of various charm hadrons based on the explanation of the experimental data of various light and strange hadrons. The p_T dependence of charm meson ratios D_s^+/D^0 and $2D_s^+/(D^0 + D^+)$ are especially selected to probe the dynamics of charm quark hadronization.

The rest of the paper is organized as follows. In Sec. II, we deduce the yield formulas and systematically study the yield ratios and multiplicities of charm hadrons in the QCM. In Sec. III, we present the p_T spectra of light, strange and charm hadrons, as well as the p_T dependence of charm meson ratios D_s^+/D^0 and $2D_s^+/(D^0 + D^+)$. Section IV summaries our work.

II. YIELD CORRELATIONS AND MULTIPLICITIES OF CHARM HADRONS IN THE QCM

In this section, we extend the formulas of hadron yields in Ref. [26] to incorporating charm hadrons in the QCM. We discuss several interesting yield ratios of charm hadrons which can reflect different properties in their production and predict the midrapidity hadron yields in central Pb + Pb collisions at $\sqrt{s_{NN}} = 2.76$ TeV.

A. The formalism of the hadron yield

We start with a color-neutral quark-antiquark system with N_{q_i} quarks of flavor q_i ($q_i = u,d,s,c$) and $N_{\bar{q}_i}$ antiquarks of flavor $\bar{q}_i$ ($\bar{q}_i = \bar{u},\bar{d},\bar{s},\bar{c}$). All these quarks and antiquarks hadronize via the quark combination. The momentum distributions $f_{M_j}(p; N_{q_i}, N_{\bar{q}_i})$ and $f_{B_j}(p; N_{q_i}, N_{\bar{q}_i})$ for the directly

*shaofl@mail.sdu.edu.cn

 ©2015 American Physical Society

produced mesons M_j and baryons B_j are given by

$$f_{M_j}(p;N_{q_i},N_{\bar{q}_i}) = \sum_{q_1\bar{q}_2}\int dp_1dp_2 N_{q_1\bar{q}_2} f^{(n)}_{q_1\bar{q}_2}(p_1,p_2;N_{q_i},N_{\bar{q}_i})\mathcal{R}_{M_j,q_1\bar{q}_2}(p,p_1,p_2;N_{q_i},N_{\bar{q}_i}), \tag{1}$$

$$f_{B_j}(p;N_{q_i},N_{\bar{q}_i}) = \sum_{q_1q_2q_3}\int dp_1dp_2dp_3 N_{q_1q_2q_3} f^{(n)}_{q_1q_2q_3}(p_1,p_2,p_3;N_{q_i},N_{\bar{q}_i})\mathcal{R}_{B_j,q_1q_2q_3}(p,p_1,p_2,p_3;N_{q_i},N_{\bar{q}_i}), \tag{2}$$

where $f^{(n)}_{q_1\bar{q}_2}$ and $f^{(n)}_{q_1q_2q_3}$ are the normalized two- and three-particle joint momentum distributions for $(q_1\bar{q}_2)$ and $(q_1q_2q_3)$, respectively. $N_{q_1\bar{q}_2} = N_{q_1}N_{\bar{q}_2}$ is the number of all the possible $(q_1\bar{q}_2)$'s in the system. $N_{q_1q_2q_3}$ is the number of all the possible $(q_1q_2q_3)$'s, satisfying $N_{q_1q_2q_3} = N_{q_1}N_{q_2}N_{q_3}$ for $q_1 \neq q_2 \neq q_3$, $N_{q_1q_2q_3} = N_{q_1}(N_{q_1}-1)N_{q_3}$ for $q_1 = q_2 \neq q_3$, and $N_{q_1q_2q_3} = N_{q_1}(N_{q_1}-1)(N_{q_1}-2)$ for $q_1 = q_2 = q_3$. Kernel functions $\mathcal{R}_{M_j,q_1\bar{q}_2}$ and $\mathcal{R}_{B_j,q_1q_2q_3}$ stand for the probability density for q_1 and $\bar{q}_2$ with momenta p_1 and p_2 to combine into a meson M_j of momentum p and that for q_1, q_2, and q_3 with momenta p_1, p_2, and p_3 to coalescence into a baryon B_j of momentum p. Integrating over p from Eqs. (1) and (2), we can obtain the average numbers of the directly produced mesons M_j and baryons B_j as

$$\overline{N}_{M_j}(N_{q_i},N_{\bar{q}_i}) = \sum_{q_1\bar{q}_2}\int dpdp_1dp_2 N_{q_1\bar{q}_2} f^{(n)}_{q_1\bar{q}_2}(p_1,p_2;N_{q_i},N_{\bar{q}_i})\mathcal{R}_{M_j,q_1\bar{q}_2}(p,p_1,p_2;N_{q_i},N_{\bar{q}_i}), \tag{3}$$

$$\overline{N}_{B_j}(N_{q_i},N_{\bar{q}_i}) = \sum_{q_1q_2q_3}\int dpdp_1dp_2dp_3 N_{q_1q_2q_3} f^{(n)}_{q_1q_2q_3}(p_1,p_2,p_3;N_{q_i},N_{\bar{q}_i})\mathcal{R}_{B_j,q_1q_2q_3}(p,p_1,p_2,p_3;N_{q_i},N_{\bar{q}_i}). \tag{4}$$

Equations (1)–(4) are the starting point of describing the hadron production in high energy reactions based on the basic ideas of the QCM. Kernel functions $\mathcal{R}_{M_j,q_1\bar{q}_2}$ and $\mathcal{R}_{B_j,q_1q_2q_3}$ carry the dynamical information of the quark combination. In general, the momentum and the flavor dependencies of these kernel functions are coupled to each other. In that case, yields and yield correlations of different hadrons can be dependent on the way of coupling. In this paper, we do not consider such coupling effects. In contrast, in the following, we consider only a simpler case where the flavor and momentum dependencies of kernel functions are factorized, i.e.,

$$\mathcal{R}_{M_j,q_1\bar{q}_2}(p,p_1,p_2;N_{q_i},N_{\bar{q}_i}) = \mathcal{R}^{(f)}_{M_j,q_1\bar{q}_2}(N_{q_i},N_{\bar{q}_i}) \times \begin{cases} \mathcal{R}^{(p)}_{M_{l\bar{l}}}(p,p_1,p_2;N_l,N_{\bar{l}},N_q,N_{\bar{q}}) & \text{for } l-\bar{l} \text{ combination} \\ \mathcal{R}^{(p)}_{M_{l\bar{c}}}(p,p_1,p_2;N_l,N_{\bar{l}},N_q,N_{\bar{q}}) & \text{for } l-\bar{c} \text{ combination} \\ \mathcal{R}^{(p)}_{M_{c\bar{l}}}(p,p_1,p_2;N_l,N_{\bar{l}},N_q,N_{\bar{q}}) & \text{for } c-\bar{l} \text{ combination,} \end{cases} \tag{5}$$

$$\mathcal{R}_{B_j,q_1q_2q_3}(p,p_1,p_2,p_3;N_{q_i},N_{\bar{q}_i}) = \mathcal{R}^{(f)}_{B_j,q_1q_2q_3}(N_{q_i},N_{\bar{q}_i}) \times \begin{cases} \mathcal{R}^{(p)}_{B_{lll}}(p,p_1,p_2,p_3;N_l,N_{\bar{l}},N_q,N_{\bar{q}}) & \text{for } l-l-l \text{ combination} \\ \mathcal{R}^{(p)}_{B_{cll}}(p,p_1,p_2,p_3;N_l,N_{\bar{l}},N_q,N_{\bar{q}}) & \text{for } c-l-l \text{ combination.} \end{cases} \tag{6}$$

Considering the large difference in mass between c and u,d,s quarks, the combination probability between c and l may be different from that between l and l. In the above two equations, we use these different $\mathcal{R}^{(p)}_{M_{l\bar{l}}}$ and $\mathcal{R}^{(p)}_{M_{l\bar{c}}}$, etc., to denote these different combination probabilities. Here, l stands for u, d or s; N_l and $N_{\bar{l}}$ stand for the total number of u,d, and s quarks and that of $\bar{u},\bar{d}$, and $\bar{s}$ antiquarks, respectively; N_q and $N_{\bar{q}}$ stand for the total number of u,d,s,c quarks and that of $\bar{u},\bar{d},\bar{s},\bar{c}$ antiquarks in the considered quark-antiquark system. We here refer to single-charm hadrons, i.e., hadrons with charm number $c = \pm 1$, in addition to light and strange hadrons. $\mathcal{R}^{(p)}_{M_{l\bar{l}}}$ denotes the probability of l and $\bar{l}$ with momenta p_1 and p_2 to combine into a light or strange meson $M_{l\bar{l}}$ with momentum p; $\mathcal{R}^{(p)}_{M_{l\bar{c}}}$ and $\mathcal{R}^{(p)}_{M_{c\bar{l}}}$ denote the probabilities for a $(l\bar{c})$ combination and a $(c\bar{l})$ combination, respectively. $\mathcal{R}^{(p)}_{B_{lll}}$ and $\mathcal{R}^{(p)}_{B_{cll}}$ denote the probability for a (lll) with momenta p_1, p_2, and p_3 to combine to form a light or strange baryon B_{lll} with momentum p and that for a (cll) or (lcl) or (llc) with momenta p_1, p_2, and p_3 to combine to form a single-charm baryon B_{cll} with momentum p. The u,d,s,c flavor-dependent parts $\mathcal{R}^{(f)}_{M_j,q_1\bar{q}_2}$ and $\mathcal{R}^{(f)}_{B_j,q_1q_2q_3}$ present the probability for the q_1 and $\bar{q}_2$ to combine into the specified meson M_j in the case that they are known to combine into a meson and that for the q_1, q_2, and q_3 to combine into the specified baryon B_j in the case that they are known to combine into a baryon. They satisfy the normalization conditions $\sum_{M_j}\mathcal{R}^{(f)}_{M_j,q_1\bar{q}_2} = 1$ and $\sum_{B_j}\mathcal{R}^{(f)}_{B_j,q_1q_2q_3} = 1$. We further adopt the assumption of u,d,s-flavor independence of the normalized joint momentum distributions of quarks and/or antiquarks, i.e.,

$$f^{(n)}_{q_1\bar{q}_2}(p_1,p_2;N_{q_i},N_{\bar{q}_i}) = \begin{cases} f^{(n)}_{l\bar{l}}(p_1,p_2;N_l,N_{\bar{l}},N_q,N_{\bar{q}}) & q_1,q_2 = u,d,s \\ f^{(n)}_{l\bar{c}}(p_1,p_2;N_l,N_{\bar{l}},N_q,N_{\bar{q}}) & q_1 = u,d,s \quad \text{and} \quad q_2 = c \\ f^{(n)}_{c\bar{l}}(p_1,p_2;N_l,N_{\bar{l}},N_q,N_{\bar{q}}) & q_1 = c \quad \text{and} \quad q_2 = u,d,s, \end{cases} \tag{7}$$

$$f^{(n)}_{q_1q_2q_3}(p_1,p_2,p_3;N_{q_i},N_{\bar{q}_i}) = \begin{cases} f^{(n)}_{lll}(p_1,p_2,p_3;N_l,N_{\bar{l}},N_q,N_{\bar{q}}) & q_1,q_2,q_3 = u,d,s \\ f^{(n)}_{cll}(p_1,p_2,p_3;N_l,N_{\bar{l}},N_q,N_{\bar{q}}) & \text{one of } q_1,q_2,q_3 \text{ is } c. \end{cases} \tag{8}$$

With these two assumptions, we have

$$\begin{aligned}
&\overline{N}_{M_j}(N_{q_i},N_{\bar{q}_i})\\
&\quad=\sum_{q_1\bar{q}_2} N_{q_1\bar{q}_2}\mathcal{R}^{(f)}_{M_j,q_1\bar{q}_2}(N_{q_i},N_{\bar{q}_i})\\
&\qquad\times\begin{cases}\int dpdp_1dp_2 f^{(n)}_{l\bar{l}}(p_1,p_2;N_l,N_{\bar{l}},N_q,N_{\bar{q}})\mathcal{R}^{(p)}_{M_{l\bar{l}}}(p,p_1,p_2;N_l,N_{\bar{l}},N_q,N_{\bar{q}}) & \text{for light and strange mesons}\\ \int dpdp_1dp_2 f^{(n)}_{l\bar{c}}(p_1,p_2;N_l,N_{\bar{l}},N_q,N_{\bar{q}})\mathcal{R}^{(p)}_{M_{l\bar{c}}}(p,p_1,p_2;N_l,N_{\bar{l}},N_q,N_{\bar{q}}) & \text{for anti-open-charm mesons}\\ \int dpdp_1dp_2 f^{(n)}_{c\bar{l}}(p_1,p_2;N_l,N_{\bar{l}},N_q,N_{\bar{q}})\mathcal{R}^{(p)}_{M_{c\bar{l}}}(p,p_1,p_2;N_l,N_{\bar{l}},N_q,N_{\bar{q}}) & \text{for open-charm mesons,}\end{cases}
\end{aligned}\tag{9}$$

$$\begin{aligned}
&\overline{N}_{B_j}(N_{q_i},N_{\bar{q}_i})\\
&\quad=\sum_{q_1q_2q_3} N_{q_1q_2q_3}\mathcal{R}^{(f)}_{B_j,q_1q_2q_3}(N_{q_i},N_{\bar{q}_i})\\
&\qquad\times\begin{cases}\int dpdp_1dp_2dp_3 f^{(n)}_{lll}(p_1,p_2,p_3;N_l,N_{\bar{l}},N_q,N_{\bar{q}})\mathcal{R}^{(p)}_{B_{lll}}(p,p_1,p_2,p_3;N_l,N_{\bar{l}},N_q,N_{\bar{q}}) & \text{for light and strange baryons}\\ \int dpdp_1dp_2dp_3 f^{(n)}_{cll}(p_1,p_2,p_3;N_l,N_{\bar{l}},N_q,N_{\bar{q}})\mathcal{R}^{(p)}_{B_{cll}}(p,p_1,p_2,p_3;N_l,N_{\bar{l}},N_q,N_{\bar{q}}) & \text{for single-charm baryons.}\end{cases}
\end{aligned}\tag{10}$$

We, respectively, denote the integrals in Eqs. (9) and (10) to be $\gamma_{M_{l\bar{l}}}(N_l,N_{\bar{l}},N_q,N_{\bar{q}})$, $\gamma_{M_{l\bar{c}}}(N_l,N_{\bar{l}},N_q,N_{\bar{q}})$, $\gamma_{M_{c\bar{l}}}(N_l,N_{\bar{l}},N_q,N_{\bar{q}})$, $\gamma_{B_{lll}}(N_l,N_{\bar{l}},N_q,N_{\bar{q}})$, and $\gamma_{B_{cll}}(N_l,N_{\bar{l}},N_q,N_{\bar{q}})$ and obtain

$$\overline{N}_{M_j}(N_{q_i},N_{\bar{q}_i})=\sum_{q_1\bar{q}_2} N_{q_1\bar{q}_2}\mathcal{R}^{(f)}_{M_j,q_1\bar{q}_2}(N_{q_i},N_{\bar{q}_i})\times\begin{cases}\gamma_{M_{l\bar{l}}}(N_l,N_{\bar{l}},N_q,N_{\bar{q}}) & \text{for light and strange mesons}\\ \gamma_{M_{l\bar{c}}}(N_l,N_{\bar{l}},N_q,N_{\bar{q}}) & \text{for anti-open-charm mesons}\\ \gamma_{M_{c\bar{l}}}(N_l,N_{\bar{l}},N_q,N_{\bar{q}}) & \text{for open-charm mesons,}\end{cases}\tag{11}$$

$$\overline{N}_{B_j}(N_{q_i},N_{\bar{q}_i})=\sum_{q_1q_2q_3} N_{q_1q_2q_3}\mathcal{R}^{(f)}_{B_j,q_1q_2q_3}(N_{q_i},N_{\bar{q}_i})\times\begin{cases}\gamma_{B_{lll}}(N_l,N_{\bar{l}},N_q,N_{\bar{q}}) & \text{for light and strange baryons}\\ \gamma_{B_{cll}}(N_l,N_{\bar{l}},N_q,N_{\bar{q}}) & \text{for single-charm baryons.}\end{cases}\tag{12}$$

Summing over different species of light and strange mesons, anti-open-charm mesons, open-charm mesons, light and strange baryons, single-charm baryons, respectively, we obtain the average numbers of all the light and strange mesons $\overline{N}_{M_{l\bar{l}}}$, anti-open-charm mesons $\overline{N}_{M_{l\bar{c}}}$, open-charm mesons $\overline{N}_{M_{c\bar{l}}}$, light and strange baryons $\overline{N}_{B_{lll}}$, and single-charm baryons $\overline{N}_{B_{cll}}$ as follows:

$$\overline{N}_{M_{l\bar{l}}}(N_l,N_{\bar{l}},N_q,N_{\bar{q}})=N_{l\bar{l}}\gamma_{M_{l\bar{l}}}(N_l,N_{\bar{l}},N_q,N_{\bar{q}}),\tag{13}$$

$$\overline{N}_{M_{l\bar{c}}}(N_l,N_{\bar{l}},N_q,N_{\bar{q}})=N_{l\bar{c}}\gamma_{M_{l\bar{c}}}(N_l,N_{\bar{l}},N_q,N_{\bar{q}}),\tag{14}$$

$$\overline{N}_{M_{c\bar{l}}}(N_l,N_{\bar{l}},N_q,N_{\bar{q}})=N_{c\bar{l}}\gamma_{M_{c\bar{l}}}(N_l,N_{\bar{l}},N_q,N_{\bar{q}}),\tag{15}$$

$$\overline{N}_{B_{lll}}(N_l,N_{\bar{l}},N_q,N_{\bar{q}})=N_{lll}\gamma_{B_{lll}}(N_l,N_{\bar{l}},N_q,N_{\bar{q}}),\tag{16}$$

$$\overline{N}_{B_{cll}}(N_l,N_{\bar{l}},N_q,N_{\bar{q}})=N_{cll}\gamma_{B_{cll}}(N_l,N_{\bar{l}},N_q,N_{\bar{q}}),\tag{17}$$

where $N_{l\bar{l}}=N_lN_{\bar{l}}$, $N_{l\bar{c}}=N_lN_{\bar{c}}$, $N_{c\bar{l}}=N_cN_{\bar{l}}$, $N_{lll}=N_l(N_l-1)(N_l-2)$, and $N_{cll}=N_cN_l(N_l-1)$. Substitute Eqs. (13)–(17) into Eqs. (11) and (12), the average number of a specified meson M_j and that of a specified baryon B_j are given by

$$\begin{aligned}
\overline{N}_{M_j}(N_{q_i},N_{\bar{q}_i})&=\sum_{q_1\bar{q}_2} N_{q_1\bar{q}_2}\mathcal{R}^{(f)}_{M_j,q_1\bar{q}_2}(N_{q_i},N_{\bar{q}_i})\times\begin{cases}\frac{1}{N_{l\bar{l}}}\overline{N}_{M_{l\bar{l}}}(N_l,N_{\bar{l}},N_q,N_{\bar{q}})\\ \frac{1}{N_{l\bar{c}}}\overline{N}_{M_{l\bar{c}}}(N_l,N_{\bar{l}},N_q,N_{\bar{q}})\\ \frac{1}{N_{c\bar{l}}}\overline{N}_{M_{c\bar{l}}}(N_l,N_{\bar{l}},N_q,N_{\bar{q}})\end{cases}\\
&=\begin{cases}C_{M_j}\frac{N_{l_1\bar{l}_2}}{N_{l\bar{l}}}\overline{N}_{M_{l\bar{l}}}(N_l,N_{\bar{l}},N_q,N_{\bar{q}}) & \text{for light and strange mesons}\\ C_{M_j}\frac{N_{l_1\bar{c}}}{N_{l\bar{c}}}\overline{N}_{M_{l\bar{c}}}(N_l,N_{\bar{l}},N_q,N_{\bar{q}}) & \text{for anti-open-charm mesons}\\ C_{M_j}\frac{N_{c\bar{l}_2}}{N_{c\bar{l}}}\overline{N}_{M_{c\bar{l}}}(N_l,N_{\bar{l}},N_q,N_{\bar{q}}) & \text{for open-charm mesons,}\end{cases}
\end{aligned}\tag{18}$$

$$\begin{aligned}
\overline{N}_{B_j}(N_{q_i},N_{\bar{q}_i})&=\sum_{q_1q_2q_3} N_{q_1q_2q_3}\mathcal{R}^{(f)}_{B_j,q_1q_2q_3}(N_{q_i},N_{\bar{q}_i})\times\begin{cases}\frac{1}{N_{lll}}\overline{N}_{B_{lll}}(N_l,N_{\bar{l}},N_q,N_{\bar{q}})\\ \frac{1}{N_{cll}}\overline{N}_{B_{cll}}(N_l,N_{\bar{l}},N_q,N_{\bar{q}})\end{cases}\\
&=\begin{cases}N_{\text{iter}}C_{B_j}\frac{N_{l_1l_2l_3}}{N_{lll}}\overline{N}_{B_{lll}}(N_l,N_{\bar{l}},N_q,N_{\bar{q}}) & \text{for light and strange baryons}\\ N_{\text{iter}}C_{B_j}\frac{N_{cl_1l_2}}{N_{cll}}\overline{N}_{B_{cll}}(N_l,N_{\bar{l}},N_q,N_{\bar{q}}) & \text{for single-charm baryons,}\end{cases}
\end{aligned}\tag{19}$$

where l_i denotes u,d,s and $\bar{l}_i$ denotes $\bar{u}$,$\bar{d}$,$\bar{s}$. The flavor-dependent parts $\mathcal{R}^{(f)}_{M_j,q_1\bar{q}_2}$ and $\mathcal{R}^{(f)}_{B_j,q_1q_2q_3}$ have to guarantee the flavor conservation during the combination process, so they contain the Kronecker δ's and factors C_{M_j} and C_{B_j}, e.g., $\mathcal{R}^{(f)}_{\rho^+,q_1\bar{q}_2} = C_{\rho^+}\delta_{q_1,u}\delta_{\bar{q}_2,\bar{d}}$. Recalling that $\mathcal{R}^{(f)}_{M_j,q_1\bar{q}_2}$ presents the probability for q_1 and $\bar{q}_2$ to combine into a specified meson M_j under the condition that they are known to form a meson. Although we cannot prove it, it is very unlikely that this probability is still sensitive to the environment. We therefore consider the simplified case where C_{M_j} is independent of N_{q_i} or $N_{\bar{q}_i}$. In the case when only $J^P = 0^-$ and 1^- mesons and $J^P = (1/2)^+$ and $(3/2)^+$ baryons are considered, we get

$$C_{M_j} = \begin{cases} 1/(1+R_{V/P}) & \text{for} \quad J^P = 0^- \text{ mesons} \\ R_{V/P}/(1+R_{V/P}) & \text{for} \quad J^P = 1^- \text{ mesons,} \end{cases} \tag{20}$$

and

$$C_{B_j} = \begin{cases} R_{O/D}/(1+R_{O/D}) & \text{for} \quad J^P = (1/2)^+ \text{ baryons} \\ 1/(1+R_{O/D}) & \text{for} \quad J^P = (3/2)^+ \text{ baryons,} \end{cases} \tag{21}$$

except that $C_\Lambda = C_{\Sigma^0} = C_{\Lambda_c^+} = C_{\Sigma_c^+} = R_{O/D}/(1+2R_{O/D})$ and $C_{\Sigma^{*0}} = C_{\Sigma_c^{*+}} = 1/(1+2R_{O/D})$. The factors $R_{V/P}$ and $R_{O/D}$ are the relative production ratio of vector to pseudoscalar mesons and that of octet to decuplet baryons with the same flavor compositions, and they have been determined to be 3 and 2, respectively, in light and strange sectors [33,34]. $N_{\rm iter}$ stands for the number of possible iterations of $q_1q_2q_3$. For light and strange baryons, it is taken to be 1, 3, and 6 for three identical flavor, two different flavor, and three different flavor cases, respectively. For single-charm baryons, it is taken to be 1 and 2 for two different flavor and three different flavor cases, respectively, because the iterations resulted from c quark are absorbed by $\overline{N}_{B_{cll}}$.

For a reaction at a given energy, the average numbers of quarks of different flavors $\langle N_{q_i}\rangle$ and those of antiquarks of different flavors $\langle N_{\bar{q}_i}\rangle$ are fixed while N_{q_i} and $N_{\bar{q}_i}$ follow a certain distribution. In this work, we focus on the midrapidity region at high LHC energy where the influence of net quarks is negligible [35]. We suppose a polynomial distribution for both the numbers of u, d, and s quarks at a given N_l and the numbers of $\bar{u}$, $\bar{d}$, and $\bar{s}$ at a given $N_{\bar{l}}$ with the prior probabilities $p_u = p_d = p_{\bar{u}} = p_{\bar{d}} = 1/(2+\lambda_s)$, $p_s = p_{\bar{s}} = \lambda_s/(2+\lambda_s)$. Here, we introduce λ_s to denote the production suppression of strange quarks. Averaging over this distribution, Eqs. (18) and (19) become

$$\overline{N}_{M_j}(N_l,N_{\bar{l}},N_q,N_{\bar{q}}) = \begin{cases} C_{M_j}\ p_{l_1}p_{\bar{l}_2}\overline{N}_{M_{l\bar{l}}}(N_l,N_{\bar{l}},N_q,N_{\bar{q}}) & \text{for} \quad \text{light and strange mesons} \\ C_{M_j}\ p_{l_1}\overline{N}_{M_{l\bar{c}}}(N_l,N_{\bar{l}},N_q,N_{\bar{q}}) & \text{for} \quad \text{anti-open-charm mesons} \\ C_{M_j}\ p_{\bar{l}_2}\overline{N}_{M_{c\bar{l}}}(N_l,N_{\bar{l}},N_q,N_{\bar{q}}) & \text{for} \quad \text{open-charm mesons,} \end{cases} \tag{22}$$

$$\overline{N}_{B_j}(N_l,N_{\bar{l}},N_q,N_{\bar{q}}) = \begin{cases} N_{\rm iter}C_{B_j}\ p_{l_1}p_{l_2}p_{l_3}\overline{N}_{B_{lll}}(N_l,N_{\bar{l}},N_q,N_{\bar{q}}) & \text{for light and strange baryons} \\ N_{\rm iter}C_{B_j}\ p_{l_1}p_{l_2}\overline{N}_{B_{cll}}(N_l,N_{\bar{l}},N_q,N_{\bar{q}}) & \text{for single-charm baryons.} \end{cases} \tag{23}$$

We should also consider the fluctuations of N_l, $N_{\bar{l}}$, N_q, and $N_{\bar{q}}$ in the given kinematic region. By averaging over this fluctuation distribution with the fixed $\langle N_l\rangle$, $\langle N_{\bar{l}},\rangle$ $\langle N_q\rangle$, and $\langle N_{\bar{q}}\rangle$, we have

$$\langle N_{M_j}\rangle(\langle N_l\rangle,\langle N_{\bar{l}}\rangle,\langle N_q\rangle,\langle N_{\bar{q}}\rangle) = \begin{cases} C_{M_j}\ p_{l_1}p_{\bar{l}_2}\langle N_{M_{l\bar{l}}}\rangle(\langle N_l\rangle,\langle N_{\bar{l}}\rangle,\langle N_q\rangle,\langle N_{\bar{q}}\rangle) & \text{for} \quad \text{light and strange mesons} \\ C_{M_j}\ p_{l_1}\langle N_{M_{l\bar{c}}}\rangle(\langle N_l\rangle,\langle N_{\bar{l}}\rangle,\langle N_q\rangle,\langle N_{\bar{q}}\rangle) & \text{for} \quad \text{anti-open-charm mesons} \\ C_{M_j}\ p_{\bar{l}_2}\langle N_{M_{c\bar{l}}}\rangle(\langle N_l\rangle,\langle N_{\bar{l}}\rangle,\langle N_q\rangle,\langle N_{\bar{q}}\rangle) & \text{for} \quad \text{open-charm mesons,} \end{cases} \tag{24}$$

$$\langle N_{B_j}\rangle(\langle N_l\rangle,\langle N_{\bar{l}}\rangle,\langle N_q\rangle,\langle N_{\bar{q}}\rangle) = \begin{cases} N_{\rm iter}C_{B_j}\ p_{l_1}p_{l_2}p_{l_3}\langle N_{B_{lll}}\rangle(\langle N_l\rangle,\langle N_{\bar{l}}\rangle,\langle N_q\rangle,\langle N_{\bar{q}}\rangle) & \text{for} \quad \text{light and strange baryons} \\ N_{\rm iter}C_{B_j}\ p_{l_1}p_{l_2}\langle N_{B_{cll}}\rangle(\langle N_l\rangle,\langle N_{\bar{l}}\rangle,\langle N_q\rangle,\langle N_{\bar{q}}\rangle) & \text{for single-charm baryons,} \end{cases} \tag{25}$$

where $\langle N_{M_{l\bar{l}}}\rangle$, $\langle N_{M_{l\bar{c}}}\rangle$, $\langle N_{M_{c\bar{l}}}\rangle$, $\langle N_{B_{lll}}\rangle$, and $\langle N_{B_{cll}}\rangle$ stand, respectively, for the average total numbers of the light and strange mesons, anti-open-charm mesons, open-charm mesons, light and strange baryons, and single-charm baryons produced in the combination process. So far, we obtain the yield formulas of different directly produced light, strange and single-charm hadrons, and some of them are listed in the middle column of Table I.

Finally, we incorporate the decay contributions of short-lived hadrons to obtain

$$\langle N^f_{h_j}\rangle = \langle N_{h_j}\rangle + \sum_{i\neq j} Br(h_i \to h_j)\langle N_{h_i}\rangle, \tag{26}$$

where the superscript f denotes final hadrons. Decay branch ratio $Br(h_i \to h_j)$ is given by the Particle Data Group [36]. We include these contributions from strong and electromagnetic decays for light and strange hadrons and only consider the decay of D^* mesons for D and Σ_c and Σ_c^* baryon decays for Λ_c^+. The small decay contributions from charm hadrons for light and strange hadrons are ignored. Some of the results for final hadrons are listed in the final column of Table I. For π^+, we have

$$\begin{aligned} \langle N^f_{\pi^+}\rangle = {} & \frac{1.71+2.91R_{V/P}}{1+R_{V/P}}p_u^2\langle N_{M_{l\bar{l}}}\rangle + \frac{0.49+0.16R_{V/P}}{1+R_{V/P}}p_s^2\langle N_{M_{l\bar{l}}}\rangle + \frac{4}{3}\frac{R_{V/P}}{1+R_{V/P}}p_up_s\langle N_{M_{l\bar{l}}}\rangle \\ & + \left(\frac{5.64}{1+R_{O/D}} + \frac{0.70}{1+2R_{O/D}}\right)p_u^2p_s\langle N_{B_{lll}}\rangle + \frac{4}{1+R_{O/D}}p_up_s^2\langle N_{B_{lll}}\rangle + \frac{4+2R_{O/D}}{1+R_{O/D}}p_u^3\langle N_{B_{lll}}\rangle. \end{aligned} \tag{27}$$

TABLE I. Yields of different light, strange, and single-charm hadrons in the QCM. The middle column is for the directly produced hadrons and those including the strong and electromagnetic (S&EM) decay contributions are in the final column.

Hadrons	Directly produced	With S&EM decays
D_s^+	$\frac{1}{1+R_{V/P}} p_s \langle N_{M_{c\bar{l}}} \rangle$	$p_s \langle N_{M_{c\bar{l}}} \rangle$
Λ_c^+	$\frac{2R_{O/D}}{1+2R_{O/D}} p_u^2 \langle N_{B_{cll}} \rangle$	$4p_u^2 \langle N_{B_{cll}} \rangle$
D^0	$\frac{1}{1+R_{V/P}} p_u \langle N_{M_{c\bar{l}}} \rangle$	$\frac{1+1.677R_{V/P}}{1+R_{V/P}} p_u \langle N_{M_{c\bar{l}}} \rangle$
D^+	$\frac{1}{1+R_{V/P}} p_u \langle N_{M_{c\bar{l}}} \rangle$	$\frac{1+0.323R_{V/P}}{1+R_{V/P}} p_u \langle N_{M_{c\bar{l}}} \rangle$
D^{*+}	$\frac{R_{V/P}}{1+R_{V/P}} p_u \langle N_{M_{c\bar{l}}} \rangle$	$\frac{R_{V/P}}{1+R_{V/P}} p_u \langle N_{M_{c\bar{l}}} \rangle$
D^{*0}	$\frac{R_{V/P}}{1+R_{V/P}} p_u \langle N_{M_{c\bar{l}}} \rangle$	$\frac{R_{V/P}}{1+R_{V/P}} p_u \langle N_{M_{c\bar{l}}} \rangle$
D_s^{*+}	$\frac{R_{V/P}}{1+R_{V/P}} p_s \langle N_{M_{c\bar{l}}} \rangle$	$\frac{R_{V/P}}{1+R_{V/P}} p_s \langle N_{M_{c\bar{l}}} \rangle$
p	$\frac{3R_{O/D}}{1+R_{O/D}} p_u^3 \langle N_{B_{lll}} \rangle$	$4p_u^3 \langle N_{B_{lll}} \rangle$
n	$\frac{3R_{O/D}}{1+R_{O/D}} p_u^3 \langle N_{B_{lll}} \rangle$	$4p_u^3 \langle N_{B_{lll}} \rangle$
Ξ^-	$\frac{3R_{O/D}}{1+R_{O/D}} p_u p_s^2 \langle N_{B_{lll}} \rangle$	$3p_u p_s^2 \langle N_{B_{lll}} \rangle$
Ω^-	$p_s^3 \langle N_{B_{lll}} \rangle$	$p_s^3 \langle N_{B_{lll}} \rangle$
K^+	$\frac{1}{1+R_{V/P}} p_u p_s \langle N_{M_{l\bar{l}}} \rangle$	$p_u p_s (1 + \frac{0.49R_{V/P}}{1+R_{V/P}} \lambda_s) \langle N_{M_{l\bar{l}}} \rangle$
K^0	$\frac{1}{1+R_{V/P}} p_u p_s \langle N_{M_{l\bar{l}}} \rangle$	$p_u p_s (1 + \frac{0.34R_{V/P}}{1+R_{V/P}} \lambda_s) \langle N_{M_{l\bar{l}}} \rangle$
ϕ	$\frac{R_{V/P}}{1+R_{V/P}} p_s^2 \langle N_{M_{l\bar{l}}} \rangle$	$\frac{R_{V/P}}{1+R_{V/P}} p_s^2 \langle N_{M_{l\bar{l}}} \rangle$
Λ	$\frac{6R_{O/D}}{1+2R_{O/D}} p_u^2 p_s \langle N_{B_{lll}} \rangle$	$(\frac{5.30+12R_{O/D}}{1+2R_{O/D}} + \frac{5.64}{1+R_{O/D}}) p_u^2 p_s \langle N_{B_{lll}} \rangle$

The results for antihadrons are equal to those of the corresponding hadrons because of the negligible net quarks. Because we ignore the very small decay contributions from charm hadrons, the yield formulas for light and strange hadrons obtained here are the same as those in our previous work [26].

B. Yield correlations of charm hadrons

From the results in Sec. II A, we get that the yields of identified hadrons depend on several physical parameters, e.g., $R_{V/P}$, λ_s, $\langle N_{M_{c\bar{l}}} \rangle$, and $\langle N_{B_{cll}} \rangle$, etc., while the yield ratios between different single-charm hadrons or between single-charm hadrons and light and strange hadrons depend on less or even no parameters. In the following, we study these ratios one by one.

First, we build multihadron yield correlations independent of any parameters, such as

$$
\begin{aligned}
C_1 &\equiv \frac{\langle N_{\Xi^-}^f \rangle \left(\langle N_{D^0}^f \rangle + \langle N_{D^+}^f \rangle \right)^2}{\langle N_p^f \rangle \langle N_{D_s^+}^f \rangle^2} = 3, \\
C_2 &\equiv \frac{\langle N_{D_s^+}^f \rangle \langle N_{\Xi^-}^f \rangle}{\left(\langle N_{D^0}^f \rangle + \langle N_{D^+}^f \rangle \right) \langle N_{\Omega^-}^f \rangle} = \frac{3}{2}, \\
C_3 &\equiv \frac{\langle N_{\Omega^-}^f \rangle \left(\langle N_{D^0}^f \rangle + \langle N_{D^+}^f \rangle \right)^3}{\langle N_p^f \rangle \langle N_{D_s^+}^f \rangle^3} = 2.
\end{aligned}
\tag{28}
$$

The constant values for these correlations are obtained from the basic ideas of the combination mechanism with the two assumptions. They can be used for the first test of the QCM. In other hadronization models, e.g., in the thermal model, they are not constants but depend on the chemical freeze-out temperature T_C and masses of different hadrons. We use the thermal model in Ref. [17] to calculate C_1, C_2, and C_3 at different T_C. Only $J^P = 0^-$ and 1^- mesons and $J^P = (1/2)^+$ and $(3/2)^+$ baryons are included. The calculated results are listed in Table II. We find that the prediction differences between QCM and the thermal model for C_1 and C_3 are significant while that for C_2 is relatively small. Future experimental data are expected to test these two different predictions.

TABLE II. Thermal model predictions for C_1, C_2, and C_3 at different input values of T_C.

T_C (MeV)	150	160	165	170	180
C_1	1.46	1.53	1.56	1.60	1.66
C_2	1.64	1.53	1.48	1.44	1.37
C_3	0.89	1.00	1.06	1.11	1.21

Second, ratios of D^* and D mesons that only depend on one parameter $R_{V/P}$, such as

$$
\begin{aligned}
\frac{2\langle N_{D^{*+}}^f \rangle}{\langle N_{D^0}^f \rangle + \langle N_{D^+}^f \rangle} &= \frac{R_{V/P}}{1+R_{V/P}}, \\
\frac{\langle N_{D^{*+}}^f \rangle}{\langle N_{D^0}^f \rangle} &= \frac{R_{V/P}}{1+1.677R_{V/P}}, \\
\frac{\langle N_{D^{*+}}^f \rangle}{\langle N_{D^+}^f \rangle} &= \frac{R_{V/P}}{1+0.323R_{V/P}}, \\
\frac{\langle N_{D^0}^f \rangle}{\langle N_{D^+}^f \rangle} &= \frac{1+1.677R_{V/P}}{1+0.323R_{V/P}}.
\end{aligned}
\tag{29}
$$

The first two ratios are sensitive to $R_{V/P}$ in the region where $R_{V/P} < 1$, and the last two are sensitive to $R_{V/P}$ in the whole region where $R_{V/P} \leqslant 3$. By the measurement of these four ratios we can quantify $R_{V/P}$, which is helpful for the understanding of the effects of spin interactions during hadronization. Because the mass discrepancy between D^* and D is much smaller than that in light and strange hadrons, one could expect that D^* is not suppressed relative to D and $R_{V/P}$ should approach 3 by counting the spin degree of freedom in the charm sector. The current data of D^{*+}/D^0 in pp reactions at LHC [37] constrain a rough value region of $R_{V/P}$ (0.7–3), if one believes that $R_{V/P}$ is the same in pp and AA collisions [27,38]. Here we take $R_{V/P} = 3$ and present our predictions for the above ratios in Table III. Predictions from the thermal model [39] are also listed for comparisons.

Third, ratios between D_s and D mesons that relate with the strangeness suppression factor λ_s, e.g.,

$$
\begin{aligned}
\frac{2\langle N_{D_s^+}^f \rangle}{\langle N_{D^0}^f \rangle + \langle N_{D^+}^f \rangle} &= \lambda_s, \qquad \frac{\langle N_{D_s^+}^f \rangle}{\langle N_{D^0}^f \rangle} = \frac{1+R_{V/P}}{1+1.677R_{V/P}} \lambda_s, \\
\frac{\langle N_{D_s^+}^f \rangle}{\langle N_{D^+}^f \rangle} &= \frac{1+R_{V/P}}{1+0.323R_{V/P}} \lambda_s.
\end{aligned}
\tag{30}
$$

TABLE III. Yield ratios of different single-charm hadrons. The second column is the predictions from the thermal model [39] and the last column is those from the QCM.

Correlations	Thermal model	QCM
$2\langle N^f_{D^{*+}}\rangle/(\langle N^f_{D^0}\rangle+\langle N^f_{D^+}\rangle)$	0.543	0.75
$\langle N^f_{D^{*+}}\rangle/\langle N^f_{D^0}\rangle$	0.387	0.50
$\langle N^f_{D^{*+}}\rangle/\langle N^f_{D^+}\rangle$	0.911	1.52
$\langle N^f_{D^0}\rangle/\langle N^f_{D^+}\rangle$	2.353	3.06
$2\langle N^f_{D_s^+}\rangle/(\langle N^f_{D^0}\rangle+\langle N^f_{D^+}\rangle)$	0.490	0.41
$\langle N^f_{D_s^+}\rangle/\langle N^f_{D^0}\rangle$	0.349	0.27
$\langle N^f_{D_s^+}\rangle/\langle N^f_{D^+}\rangle$	0.821	0.83
$\langle N^f_{\Lambda_c^+}\rangle/(\langle N^f_{D^0}\rangle+\langle N^f_{D^+}\rangle)$	0.114	0.21
$\langle N^f_{\Lambda_c^+}\rangle/\langle N^f_{D_s^+}\rangle$	0.467	1.01

In the QCM, a charm quark captures a light or a strange antiquark to form a D meson or a D_s meson, and ratios of these D_s to D mesons carry the strangeness information of the production zone of these open-charm mesons. Therefore, these ratios can effectively probe the hadronization environment of charm quarks, i.e., inside the QGP or not. It is known that the produced bulk quark matter in Pb + Pb collisions at $\sqrt{s_{NN}} = 2.76$ TeV has the saturated strangeness, e.g., $\lambda_s = 0.41$ [26], while for the small partonic system such as that created in pp collisions the strangeness is only about 0.3 [37]. If charm quarks mainly hadronize via quark combination in the QGP, we have the numerical calculations for these three ratios and they are put in Table III. Predictions from the thermal model [39] are also listed in Table III.

Fourth, baryon-to-meson ratios, e.g.,

$$\frac{\langle N^f_{\Lambda_c^+}\rangle}{\langle N^f_{D^0}\rangle+\langle N^f_{D^+}\rangle} = \frac{2}{2+\lambda_s}\frac{\langle N_{B_{cll}}\rangle}{\langle N_{M_{c\bar{l}}}\rangle}, \qquad \frac{\langle N^f_{\Lambda_c^+}\rangle}{\langle N^f_{D_s^+}\rangle} = \frac{4}{\lambda_s(2+\lambda_s)}\frac{\langle N_{B_{cll}}\rangle}{\langle N_{M_{c\bar{l}}}\rangle}. \tag{31}$$

These ratios can effectively reflect the baryon-meson competition in the charm sector. We suppose that the baryon-meson competition in the charm sector is the same as that in light and strange sectors, and have $\langle N_{B_{cll}}\rangle/\langle N_{M_{c\bar{l}}}\rangle = 3\langle N_{B_{lll}}\rangle/\langle N_{M_{l\bar{l}}}\rangle$. With the parametrization $\langle N_{B_{lll}}\rangle/\langle N_{M_{l\bar{l}}}\rangle = 1/12$ in Ref. [26], we predict these two ratios and put them in Table III. Predictions from the thermal model [39] are also listed in Table III.

These different kinds of correlations discussed above can effectively reflect the properties of charm hadron production from different aspects. They can be used to cross-check the charm quark hadronization mechanism in AA collision at LHC.

C. Predictions for charm hadron yields

Now we turn to the predictions of the midrapidity yields dN/dy of various hadrons in central Pb + Pb collisions at $\sqrt{s_{NN}} = 2.76$ TeV. From Table I, one can see that the yields of different hadrons depend on these quantities: p_u, p_s, $dN_{M_{l\bar{l}}}/dy$, $dN_{M_{c\bar{l}}}/dy$, $dN_{B_{lll}}/dy$, and $dN_{B_{cll}}/dy$. We need three inputs to determine these quantities, i.e., λ_s, the rapidity density of all light and strange quarks dN_l/dy and $\lambda_c \equiv \frac{dN_c}{dy}/\frac{dN_l}{dy}$. λ_s determines p_u and p_s uniquely, and it was determined to be 0.41 [26]. The quark number conservation gives $\frac{dN_{M_{l\bar{l}}}}{dy} + \frac{dN_{M_{l\bar{c}}}}{dy} + 3\frac{dN_{B_{lll}}}{dy} + 2\frac{dN_{B_{cll}}}{dy} = \frac{dN_l}{dy}$ where the very small part of light and strange quarks going into double-charm baryons is ignored. Using the relations $\frac{dN_{M_{c\bar{l}}}}{dy}/\frac{dN_{M_{l\bar{l}}}}{dy} = \lambda_c$ and $\frac{dN_{B_{cll}}}{dy}/\frac{dN_{B_{lll}}}{dy} = 3\lambda_c$, and the parametrization $\frac{dN_{B_{lll}}}{dy}/\frac{dN_{M_{l\bar{l}}}}{dy} = 1/12$ [26], $dN_{M_{l\bar{l}}}/dy$, $dN_{M_{c\bar{l}}}/dy$, $dN_{B_{lll}}/dy$, and $dN_{B_{cll}}/dy$ can be obtained by λ_c and dN_l/dy. The rapidity density of all light and strange quarks is fixed to be $\frac{dN_l}{dy} = \frac{2.162}{2}\frac{dN_{ch}}{d\eta} \approx 1731$ [40,41] by fitting the measured pseudorapidity density of charged particles. λ_c related to the charm quark number $\frac{dN_c}{dy} = \lambda_c\frac{dN_l}{dy}$ is the key input for predictions of charm hadron yields.

Charm quarks produced at LHC mainly come from two stages of the collision: initial hard-parton scatterings and thermal partonic interactions in the QGP. Here we first give an estimation of the charm quark number $dN_c^{\rm initial}/dy$ from initial hard-parton scatterings by extrapolating pp reaction data at LHC,

$$\frac{dN_c^{\rm initial}}{dy} = \langle T_{AA}\rangle\frac{d\sigma_c^{pp}}{dy} = \langle T_{AA}\rangle\frac{1}{R}\frac{d\sigma_{D^0}^{pp}}{dy} = 21. \tag{32}$$

Here $R = 0.54 \pm 0.05$ is the branch ratio of charm quarks into final D^0 mesons measured in e^+e^- reactions [6]. $\langle T_{AA}\rangle = 26.4 \pm 0.5$ mb^{-1} is the average nuclear overlap function calculated with the Glauber model [42]. The cross section of D^0 is $\frac{d\sigma_{D^0}^{pp}}{dy} = 0.428 \pm 0.115$ mb in pp reactions at $\sqrt{s} = 2.76$ TeV [7].

Subsequent QGP evolution stage can increase the charm quark number, but the enhancement rate $\alpha \equiv (\frac{dN_c}{dy} - \frac{dN_c^{\rm initial}}{dy})/\frac{dN_c^{\rm initial}}{dy}$ is sensitive to the evolution details such as initial temperature, charm quark mass, evolution time. The present predictions of α in literatures have large uncertainties, from 0%–100% [11–13]. Here, we choose $\alpha =$ 0%,10%,20%,40%,100% to study its influence on the yields of different hadrons. The predicted yields of various single-charm hadrons as well as light and strange hadrons are shown in Table IV, and the experimental data are from Refs. [35,43–45]. The predictions for single-charm hadron yields with the statistical hadronization model (SHM) at $dN_c/dy = 16.8$ [46] are also listed in Table IV. To make comparisons with the SHM, we also present the predictions at the same dN_c/dy. We find that the results for light and strange hadrons suffer very small influences from charm quark production and they are consistent with the available data within the experimental uncertainties except for ϕ.

The current calculations of ϕ mesons are obviously higher than the data. This is because in this paper we only consider the production of $J^P = 0^-$ and $J^P = 1^-$ mesons in the ground state. In fact, various multiquark states and/or exotic states beyond the quark model are also produced in high energy

TABLE IV. Rapidity densities dN/dy of identified hadrons in central Pb+Pb collisions at $\sqrt{s_{NN}} = 2.76$ TeV. The data are from Refs. [35,43–45]. The predictions of single-charm hadrons given by the statistical hadronization model (SHM) are also listed with parentheses [46].

Hadron	Data (SHM)	$dN_c/dy = 16.8$	$dN_c/dy = 21$ ($\alpha = 0\%$)	$dN_c/dy = 23$ ($\alpha = 10\%$)	$dN_c/dy = 25$ ($\alpha = 20\%$)	$dN_c/dy = 29$ ($\alpha = 40\%$)	$dN_c/dy = 42$ ($\alpha = 100\%$)
π^+	733 ± 54	752	749	748	747	745	739
K^+	109 ± 9	111	111	111	111	110	109
K^0_S	110 ± 10	107	106	106	106	106	105
ϕ	$13.8 \pm 0.5 \pm 1.7$	29.7	29.6	29.6	29.5	29.5	29.2
p	34 ± 3	33	32	32	32	32	32
Λ	26 ± 3	26	26	26	26	26	25
Ξ^-	$3.34 \pm 0.06 \pm 0.24$	4.11	4.10	4.09	4.09	4.07	4.04
Ω^-	$0.58 \pm 0.04 \pm 0.09$	0.56	0.56	0.56	0.56	0.56	0.55
D^+	(3.56)	2.71	3.38	3.70	4.02	4.65	6.67
D^0	(7.80)	8.31	10.4	11.3	12.3	14.2	20.4
D^{*+}	(—)	4.13	5.15	5.64	6.12	7.08	10.16
D^{*0}	(—)	4.13	5.15	5.64	6.12	7.08	10.16
D_s^+	(2.96)	2.26	2.82	3.08	3.34	3.87	5.55
Λ_c^+	(1.16)	2.29	2.85	3.12	3.38	3.92	5.62

reactions. There are two exotic hadrons $f_0(980)$ and $a_0(980)$ which are mostly relevant to the ϕ abundance. The masses of these two hadrons are close to ϕ and they also probably have the large $s\bar{s}$ content according to the newest PDG [36]. Including these two hadrons in our model will consume $s\bar{s}$ pairs in the system and introduce the competition against the ϕ formation. In our previous work [27], we have studied the yield of ϕ at top SPS and RHIC energies and the results suggested that the production of exotic hadrons should exhaust about the same number of $s\bar{s}$ pairs as that in ϕ production so that the final ϕ yields are consistent with the experimental data measured by the NA49 Collaboration and the STAR Collaboration. The rigorous calculation of ϕ yield including the exotic states is a difficult task in the current progress of the hadronization phenomenology, and is beyond the intension of the current study. Based on these considerations, we multiply the factor $1/2$ to the calculated ϕ yield in Table IV to give the rough estimation of the final ϕ yield, i.e., about 14, in central Pb + Pb collisions at $\sqrt{s_{NN}} = 2.76$ TeV. We see that this estimation agrees with the experimental data. This indicates some underlying universality of ϕ production in high energy heavy ion collisions at different collision energies.

III. p_T DEPENDENCE OF LIGHT, STRANGE, AND CHARM HADRONS

p_T spectra of identified hadrons can provide more explicit insights into quark hadronization mechanisms and detailed information on the hot and dense bulk matter created in relativistic heavy ion collisions. In the QCM, p_T spectra of various light and strange hadrons can be systematically calculated with the given p_T distributions of light and strange quarks. This is one of the main features and advantages of the QCM and has tested against the experimental data at RHIC [29,30,47–50]. In the following, we test the QCM in explaining p_T spectra of identified hadrons at LHC.

Confining ourselves to the hadron production at the midrapidity $y = 0$, the transverse momentum distributions of mesons M_j and baryons B_j can be obtained from Eqs. (1) and (2) as

$$f_{M_j}(p_T; N_{q_i}, N_{\bar{q}_i}) = \sum_{q_1\bar{q}_2} \mathcal{R}^{(f)}_{M_j,q_1\bar{q}_2}(N_{q_i}, N_{\bar{q}_i}) \int dp_{T_1} dp_{T_2} N_{q_1\bar{q}_2} f^{(n)}_{q_1\bar{q}_2}(p_{T_1}, p_{T_2}; N_{q_i}, N_{\bar{q}_i}) \mathcal{R}^{(p_T)}_{M,q_1\bar{q}_2}(p_T, p_{T_1}, p_{T_2}; N_{q_i}, N_{\bar{q}_i}), \quad (33)$$

$$f_{B_j}(p_T; N_{q_i}, N_{\bar{q}_i}) = \sum_{q_1q_2q_3} \mathcal{R}^{(f)}_{B_j,q_1q_2q_3}(N_{q_i}, N_{\bar{q}_i}) \int dp_{T_1} dp_{T_2} dp_{T_3} N_{q_1q_2q_3} f^{(n)}_{q_1q_2q_3}(p_{T_1}, p_{T_2}, p_{T_3}; N_{q_i}, N_{\bar{q}_i})$$
$$\times \mathcal{R}^{(p_T)}_{B,q_1q_2q_3}(p_T, p_{T_1}, p_{T_2}, p_{T_3}; N_{q_i}, N_{\bar{q}_i}), \quad (34)$$

where the factorization assumption was applied to the kernel functions, i.e.,

$$\mathcal{R}_{M_j,q_1\bar{q}_2}(p_T, p_{T_1}, p_{T_2}; N_{q_i}, N_{\bar{q}_i}) = \mathcal{R}^{(f)}_{M_j,q_1\bar{q}_2}(N_{q_i}, N_{\bar{q}_i}) \mathcal{R}^{(p_T)}_{M,q_1\bar{q}_2}(p_T, p_{T_1}, p_{T_2}; N_{q_i}, N_{\bar{q}_i}),$$
$$\mathcal{R}_{B_j,q_1q_2q_3}(p_T, p_{T_1}, p_{T_2}, p_{T_3}; N_{q_i}, N_{\bar{q}_i}) = \mathcal{R}^{(f)}_{B_j,q_1q_2q_3}(N_{q_i}, N_{\bar{q}_i}) \mathcal{R}^{(p_T)}_{B,q_1q_2q_3}(p_T, p_{T_1}, p_{T_2}, p_{T_3}; N_{q_i}, N_{\bar{q}_i}).$$

$\mathcal{R}^{(f)}_{M_j,q_1\bar{q}_2}$ and $\mathcal{R}^{(f)}_{B_j,q_1q_2q_3}$ are the same as those in Sec. II. $\mathcal{R}^{(p_T)}_{M,q_1\bar{q}_2}$ and $\mathcal{R}^{(p_T)}_{B,q_1q_2q_3}$ also represent the same physical meaning as those in Sec. II except for the replacement of p by p_T and further distinguishing the flavors of (anti)quarks. Such a convolution method for calculating hadron p_T spectra is widely applied in quark combination models [51,52]. Here, we focus on azimuthal

angular integrated p_T distribution, so we adopt one-dimensional combination formulas in the momentum space. $\mathcal{R}^{(p_T)}_{M,q_1\bar{q}_2}$ and $\mathcal{R}^{(p_T)}_{B,q_1q_2q_3}$ contain the dynamics of quark combination in transverse momentum space, and we first isolate this part from $\mathcal{R}^{(p_T)}_{M,q_1\bar{q}_2}$ and $\mathcal{R}^{(p_T)}_{B,q_1q_2q_3}$, e.g., for the formation of light and strange hadrons,

$$\mathcal{R}^{(p_T)}_{M,q_1\bar{q}_2}(p_T,p_{T_1},p_{T_2};N_{q_i},N_{\bar{q}_i}) = \mathcal{A}_{M,q_1\bar{q}_2}(N_{q_i},N_{\bar{q}_i})\delta(p_T - p_{T_1} - p_{T_2})\Theta(\varepsilon - |p_{T_1} - p_{T_2}|), \tag{35}$$

$$\mathcal{R}^{(p_T)}_{B,q_1q_2q_3}(p_T,p_{T_1},p_{T_2},p_{T_3};N_{q_i},N_{\bar{q}_i}) = \mathcal{A}_{B,q_1q_2q_3}(N_{q_i},N_{\bar{q}_i})\delta(p_T - p_{T_1} - p_{T_2} - p_{T_3})\Theta(\varepsilon - |p_{T_1} - p_{T_2}|) \times\Theta(\varepsilon - |p_{T_1} - p_{T_3}|)\Theta(\varepsilon - |p_{T_2} - p_{T_3}|). \tag{36}$$

Here, δ functions guarantee the transverse momentum conservation in the combination process and Θ functions represent the momentum constraints that quarks and antiquarks with similar masses combine into hadrons only when they are close to each other in momentum space. ε is a parameter of small value. $\varepsilon \to 0$ leads to the ideal equal p_T combinations. Here, we set ε to be 0.2 for light and strange hadrons. For the formation of single-charm hadrons, because of the large mass discrepancy between charm quarks and light or strange quarks, the constraint of near transverse velocity in combination may be more realistic, i.e.,

$$\mathcal{R}^{(p_T)}_{M,q_1\bar{q}_2}(p_T,p_{T_1},p_{T_2};N_{q_i},N_{\bar{q}_i}) = \mathcal{A}_{M,q_1\bar{q}_2}(N_{q_i},N_{\bar{q}_i})\delta(p_T - p_{T_1} - p_{T_2})\Theta\left(\varepsilon - \left|\frac{p_{T_1}}{m_{q_1}} - \frac{p_{T_2}}{m_{q_2}}\right|\right), \tag{37}$$

where m_{q_i} is the constituent quark mass, and $m_u = m_d = 0.34$ GeV, $m_s = 0.5$ GeV, and $m_c = 1.5$ GeV.

Apart from the momentum constraints, $\mathcal{R}^{(p_T)}_{M,q_1\bar{q}_2}$ and $\mathcal{R}^{(p_T)}_{B,q_1q_2q_3}$ involve other hadronization dynamics which is incorporated in the items $\mathcal{A}_{M,q_1\bar{q}_2}$ and $\mathcal{A}_{B,q_1q_2q_3}$. First, $\mathcal{A}_{M,q_1\bar{q}_2}$ and $\mathcal{A}_{B,q_1q_2q_3}$ are obviously dependent on the N_{q_i} and/or $N_{\bar{q}_i}$ of the system. This can be illustrated by a simple consideration. Suppose we double the number of quarks and antiquarks (i.e., the size of the quark system); yields of the produced hadrons should also be double from general principles. Therefore, $\mathcal{A}_{M,q_1\bar{q}_2}$ and $\mathcal{A}_{B,q_1q_2q_3}$ should be more or less inversely proportional to N_q and/or $N_{\bar{q}}$. In essence, this dependence is the requirement of the hadronization unitarity, i.e., the production of mesons and baryons should exhaust all quarks and antiquarks of the system after hadronization. This unitarity of hadron production in heavy ion collisions was addressed early in the ALCOR model by introducing normalization factors for every flavor quarks when describing the yields of different hadrons [53]. Second, and more important, $\mathcal{A}_{M,q_1\bar{q}_2}$ and $\mathcal{A}_{B,q_1q_2q_3}$ should involve the dynamics of baryon-meson production competition, i.e., when a quark hadronizes, whether it forms a meson by combining an antiquark or forms a baryon by combining other two quarks as momentum constraints are both satisfied in two cases. Note that these $\mathcal{A}_{M,q_1\bar{q}_2}$ and $\mathcal{A}_{B,q_1q_2q_3}$ coefficients in kernel functions are the major difference of our method from those previous well-known combination models [51,52] where the combination function depends on the overlap of the wave functions of constituent quarks with that of the hadron.

Further exploration of $\mathcal{A}_{M,q_1\bar{q}_2}$ and $\mathcal{A}_{B,q_1q_2q_3}$ must deal with these sophisticated hadronization dynamics. Here, we use a specific combination model developed by the Shandong group (SDQCM) [27,34,54] to concretize these detailed dynamics in $\mathcal{A}_{M,q_1\bar{q}_2}$ and $\mathcal{A}_{B,q_1q_2q_3}$ and realize the calculation of p_T spectra of identified hadrons via Eqs. (33) and (34). Of all the on market combination models, SDQCM is unique for its ability to consistently explain of hadron yields, rapidity spectra, and p_T spectra in relativistic heavy ion collisions [16,27,34,55]. A combination rule is designed specifically in SDQCM to describe the hadronization of the color-neutral quark-antiquark system. The main idea of the combination rule is to line up the (anti)quarks in a one-dimensional order in phase space, e.g., in longitudinal rapidity, and then let them combine into initial hadrons one by one according to this order [27,34]. Three (anti)quarks or a quark-antiquark pair in the neighborhood form a (anti)baryon or a meson, respectively. When a hadron is produced in longitudinal dimension, p_T of this hadron is subsequently calculated by the transverse combination dynamics. The combination rule automatically satisfies the unitarity of the hadronization and gives the baryon-meson competition. SDQCM predictions of hadron yields are compatible with the yield formulas in Sec. II. In addition, the decay effects of resonances on the p_T spectra of stable hadrons can be conveniently taken into account in SDQCM.

Quark joint transverse momentum distributions are necessary for the calculations of p_T distributions of hadrons. Ignoring the correlations of (anti)quarks, we have $f^{(n)}_{q_1\bar{q}_2}(p_{T_1},p_{T_2};N_{q_i},N_{\bar{q}_i}) = f^{(n)}_{q_1}(p_{T_1};N_{q_i},N_{\bar{q}_i})f^{(n)}_{\bar{q}_2}(p_{T_2};N_{q_i},N_{\bar{q}_i})$ and $f^{(n)}_{q_1q_2q_3}(p_{T_1},p_{T_2},p_{T_3};N_{q_i},N_{\bar{q}_i}) = f^{(n)}_{q_1}(p_{T_1};N_{q_i},N_{\bar{q}_i})f^{(n)}_{q_2}(p_{T_2};N_{q_i},N_{\bar{q}_i})f^{(n)}_{q_3}(p_{T_3};N_{q_i},N_{\bar{q}_i})$. For the distributions of light and strange quarks, we use a two-component parametrized pattern: $dN_{l_i}/(p_T dp_T) \propto \exp(-\sqrt{p_T^2+m_{l_i}^2}/T_{l_i}) + R_{l_i}(1+\frac{p_T}{5\text{GeV}})^{-S_{l_i}}$, the exponential item for thermal quarks at low p_T and the power-law item for shower quarks with high p_T. Parameters $(T_{l_i},S_{l_i},R_{l_i})$ for light and strange quarks are extracted by fitting the data of p_T spectra of $p+\bar{p}$ and $K^+ + K^-$, respectively. Their values are (0.31 GeV, 8.0, 0.02) for light quarks and (0.36 GeV, 8.6, 0.04) for strange quarks.

Figure 1 shows the p_T spectra of $h^\pm$, $\pi^\pm$, $K^\pm$, K^0_S, ϕ, p, $\bar{p}$, Λ, Ξ^-, and Ω^- in central Pb + Pb collisions at $\sqrt{s_{NN}} = 2.76$ TeV. The calculated results denoted by different types of lines are consistent with the experimental data denoted by different solid symbols [35,42–45,56]. Note that the calculated ϕ here is the result corrected by multiplying 1/2. We see that the exponential domain of meson spectra expands to about 4 GeV/c and that of baryons expands to about 6 GeV/c.

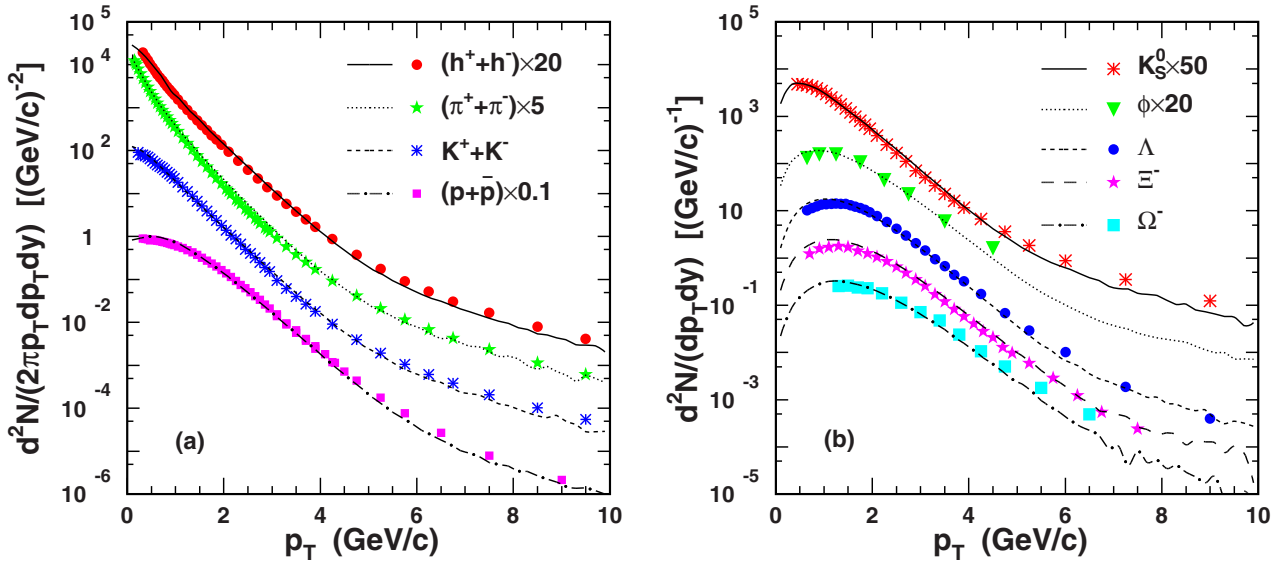

FIG. 1. (Color online) p_T distributions of light and strange hadrons in central Pb + Pb collisions at $\sqrt{s_{NN}} = 2.76$ TeV. The solid symbols are the experimental data from Refs. [35,42–45,56], and different types of lines are our results. Charged particles $h^{\pm}$ are measured in midpseudorapidity and identified hadrons are in midrapidity. $h^+ + h^-$, $\pi^+ + \pi^-$, $p + \bar{p}$, K^0_S, and ϕ are scaled by 20, 5, 0.1, 50, 20, respectively, for clear exhibitions. The calculated ϕ here is the result corrected by multiplying 1/2. Note that the data of $p + \bar{p}$ and $K^+ + K^-$ are used to extract the p_T spectra of light and strange quarks, respectively.

Compared with the data at RHIC [57], the exponential domain extends over about 2 GeV/c.

Based on the performance of the QCM in light and strange sectors, we turn to the charm sector. In the combination process of a charm quark with light and/or strange quarks to form an open charm hadron, there are two different combination scenarios, i.e., equal p_T combination and equal velocity combination, which are both possible and cannot be ruled out from the current knowledge of the nonperturbative hadronization. This will cause two different predictions for p_T distributions of charm hadrons with the same charm quark p_T spectrum. On the other hand, the calculation of the p_T spectrum for charm quarks before hadronization involves many complex factors, e.g., the nuclear shadowing on the initial hard produced charm quarks, the collisional energy loss in the QGP, and the medium-induced gluon energy loss, etc. [58–60]. The current theoretical predictions for charm quark p_T spectra have large uncertainties [58–60], which also cause the predictions that charm hadron p_T spectra have large uncertainties. In such a situation of two possible combination dynamics plus an uncertain charm quark p_T distribution, it is not so straightforward to directly test the hadronization mechanism from the experimental data of charm hadrons. In this paper, we adopt a slightly unusual study strategy, based on the philosophy that a physical charm quark p_T distribution plus a physical hadronization mechanism should give the correct, observed charm hadron p_T spectra. We extract the p_T spectrum of charm quarks from the experimental data of D^0 in the cases of equal p_T combination and equal velocity combination, respectively. Definitely, charm quark p_T spectra in these two different cases are different. Then, we predict p_T spectra of other charm hadrons in these two cases, respectively, and compare them with the available and future experimental data to check these two different combination scenarios.

The extracted charm quark p_T spectrum under the equal p_T combination is $dN_c/(p_T dp_T) \propto (p_T + 0.4\,\mathrm{GeV})^2(1 + \frac{p_T}{2.2\mathrm{GeV}})^{-8}$ while that under the equal velocity combination is $dN_c/(p_T dp_T) \propto (p_T + 0.99\,\mathrm{GeV})^2(1 + \frac{p_T}{0.87\mathrm{GeV}})^{-6.32}$. We find that the charm quark p_T spectrum extracted from the equal velocity combination is close to the theoretical prediction at LHC in a recent Ref. [59] while that from the equal p_T combination has a large difference with Ref. [59] and is close to the prediction at RHIC energies in Ref. [60]. The calculated p_T spectra of charm hadrons in these two combination scenarios are shown in Fig. 2(a). The solid lines are for the results computed in the equal p_T combination and the dashed lines for the equal velocity combination case. The solid symbols are the experimental data from Refs. [8,61]. We find that the results in two combination scenarios for D^+ and D^{*+} are nearly the same and those for D_s^+ have a relatively obvious difference in the range of $p_T > 3$ GeV.

We argue that the p_T dependence of charm meson ratios D_s^+/D^0 and $2D_s^+/(D^0 + D^+)$ are good probes to distinguish the above two different combination scenarios of charm quarks. These two ratios are essentially related to the strangeness of the production regions of charm mesons, and they are nonsensitive to the p_T distribution of charm quarks. Take D_s^+/D^0 as an example. We have the p_T dependence of D_s^+/D^0 is proportional to $f_s(\frac{p_T}{2}; N_{q_i}, N_{\bar{q}_i})/f_u(\frac{p_T}{2}; N_{q_i}, N_{\bar{q}_i})$ in the equal p_T combination and to $f_s(\frac{p_T}{4}; N_{q_i}, N_{\bar{q}_i})/f_u(\frac{p_T}{4}; N_{q_i}, N_{\bar{q}_i})$ in the equal velocity combination where we approximately use the triple mass difference in charm quarks and light or strange quarks. The similar case holds for $2D_s^+/(D^0 + D^+)$. The dot-dashed lines in Figs. 2(b) and 2(c) show the p_T dependence of the

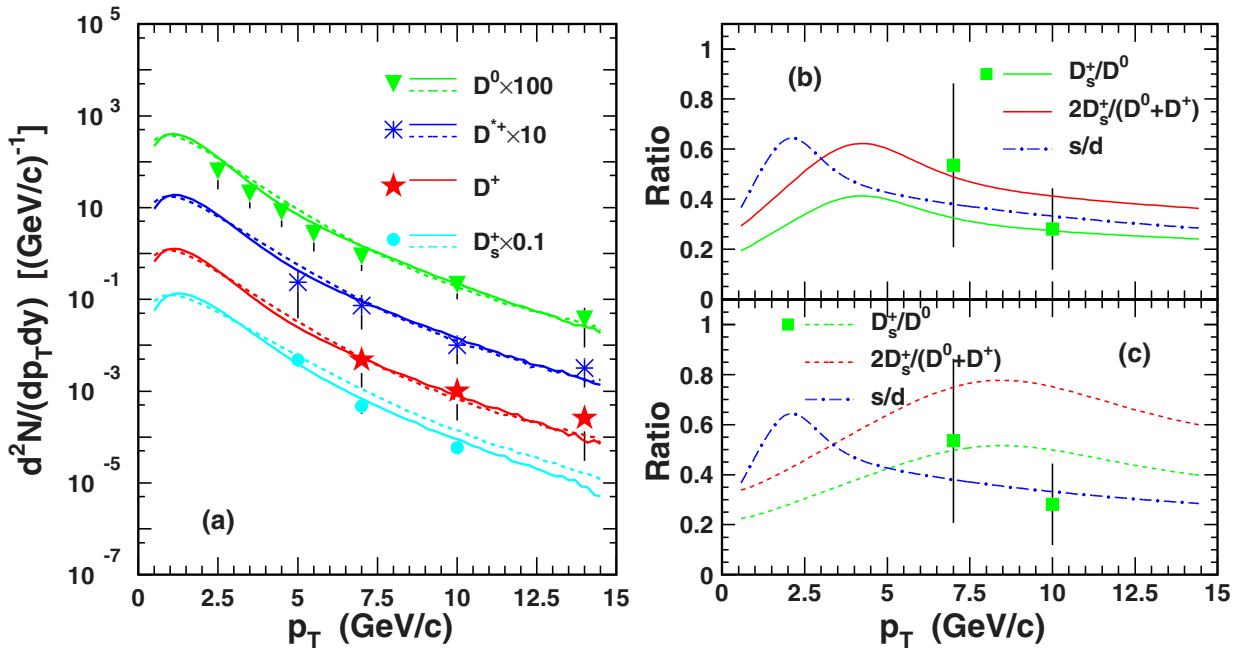

FIG. 2. (Color online) (a) p_T distributions of charm mesons and (b) charm meson ratios in equal p_T combination scenario and (c) charm meson ratios in equal velocity combination scenario at midrapidity in central Pb + Pb collisions at $\sqrt{s_{NN}} = 2.76$ TeV. The solid symbols are the experimental data from Refs. [8,61], and different lines are our results. (a) The solid lines are the results in equal p_T combination scenario and the dashed lines are the results in equal velocity combination scenario. p_T distributions for D^0, D^{*+}, and D_s^+ are scaled by 100, 10, and 0.1, respectively, for clear exhibitions. Note that the data of D^0 are used to extract the p_T spectra of charm quarks.

strangeness, i.e., the ratio of the previously extracted strange quark p_T spectrum to the down quark p_T spectrum. It rises rapidly at low p_T and reaches the peak at $p_T \approx 2$ GeV and then it decreases to a stable small value. D_s^+/D^0 and $2D_s^+/(D^0 + D^+)$ as the function of p_T should follow similar shapes by stretching out the p_T axis, but the peak position of the ratios will reflect the detailed combination dynamics of charm hadron formation. Figure 2(b) shows the results of a charm quark capturing an antiquark with an equal p_T to form a meson. The resulting D_s^+/D^0 and $2D_s^+/(D^0 + D^+)$ reach the peak at $p_T \approx 4$ GeV, and decrease to the low values at high p_T. Figure 2(c) represents the results in the case of a charm quark capturing an antiquark with an equal velocity to form a meson. The resulting D_s^+/D^0 and $2D_s^+/(D^0 + D^+)$ arrive at the peak at $p_T \approx 8$ GeV, which are quite different from those in Fig. 2(b). We note that the HIJING/BB V2.0 using the fragmentation hadronization predicts nearly no p_T dependence of these D_s^+/D ratios [62]. The future experimental data at LHC can test these different predictions.

IV. SUMMARY

We have deduced yield formulas and studied yield correlations and p_T spectra of single-charm hadrons in the QCM in central Pb + Pb collisions at $\sqrt{s_{NN}} = 2.76$ TeV. Yields of various single-charm hadrons are found to have a series of interesting correlations. Several types of yield ratios were proposed to quantify these correlations and to measure the properties of charm quark hadronization from different aspects. In addition, we systematically explained the midrapidity data of p_T spectra for $h^{\pm}$, $K^{\pm}$, K_S^0, ϕ, p, $\bar{p}$, Ξ^-, and Ω^-. We further calculated the p_T spectra of open charm mesons and found that the results agree with the available experimental data. Ratios D_s^+/D_0 and $2D_s^+/(D^0 + D^+)$ as the function of p_T are identified as good probes for the hadronization dynamics of charm quarks, and we made predictions in two different combination scenarios for the comparison with the future experimental data.

ACKNOWLEDGMENTS

The authors thank Z. T. Liang, Q. B. Xie, Q. Wang, H. J. Xu, W. Wang, and the members of the particle theory group of Shandong University for helpful discussions. This work is supported in part by the National Natural Science Foundation of China under Grants No. 11175104, No. 11305076, and No. 11247202, and by the Natural Science Foundation of Shandong Province, China under Grants No. ZR2011AM006 and No. ZR2012AM001.

[1] T. Matsui and H. Satz, Phys. Lett. B **178**, 416 (1986).
[2] H. van Hees, V. Greco, and R. Rapp, Phys. Rev. C **73**, 034913 (2006).
[3] Á. Mócsy and P. Petreczky, Phys. Rev. Lett. **99**, 211602 (2007).
[4] M. He, R. J. Fries, and R. Rapp, Phys. Rev. Lett. **110**, 112301 (2013).

[5] S. S. Adler *et al.* (PHENIX Collaboration), Phys. Rev. Lett. **94**, 082301 (2005).
[6] J. Adams *et al.* (STAR Collaboration), Phys. Rev. Lett. **94**, 062301 (2005).
[7] B. Abelev *et al.* (ALICE Collaboration), J. High Energy Phys. 07 (2012) 191.
[8] B. Abelev *et al.* (ALICE Collaboration), J. High Energy Phys. 09 (2012) 112.
[9] G. Luparello (for the ALICE Collaboration), J. Phys. Conf. Ser. **446**, 012039 (2013).
[10] H. Yang (for the ALICE Collaboration), Nucl. Phys. A **904-905**, 673c (2013).
[11] P. Lévai and R. Vogt, Phys. Rev. C **56**, 2707 (1997).
[12] J. Uphoff, O. Fochler, Z. Xu, and C. Greiner, Phys. Rev. C **82**, 044906 (2010).
[13] B. W. Zhang, C. M. Ko, and W. Liu, Phys. Rev. C **77**, 024901 (2008).
[14] K. Zhou, N. Xu, and P. F. Zhuang, arXiv:1309.7520.
[15] V. Greco, C. M. Ko, and R. Rapp, Phys. Lett. B **595**, 202 (2004).
[16] T. Yao, W. Zhou, and Q. B. Xie, Phys. Rev. C **78**, 064911 (2008).
[17] Y. Oh, C. M. Ko, S. H. Lee, and S. Yasui, Phys. Rev. C **79**, 044905 (2009).
[18] Y. P. Liu, C. Greiner, and A. Kostyuk, Phys. Rev. C **87**, 014910 (2013).
[19] M. He, R. J. Fries, and R. Rapp, Phys. Rev. C **86**, 014903 (2012).
[20] H. J. Xu, X. Dong, L. J. Ruan, Q. Wang, Z. B. Xu, and Y. F. Zhang, Phys. Rev. C **89**, 024905 (2014).
[21] R. C. Hwa, Phys. Rev. D **51**, 85 (1995).
[22] J. C. Anjos, J. Magnin, and G. Herrera, Phys. Lett. B **523**, 29 (2001).
[23] E. Braaten, Y. Jia, and T. Mehen, Phys. Rev. Lett. **89**, 122002 (2002).
[24] R. Rapp and E. V. Shuryak, Phys. Rev. D **67**, 074036 (2003).
[25] T. Mehen, J. Phys. G **30**, S295 (2004).
[26] R. Q. Wang, F. L. Shao, J. Song, Q. B. Xie, and Z. T. Liang, Phys. Rev. C **86**, 054906 (2012).
[27] C. E. Shao, J. Song, F. L. Shao, and Q. B. Xie, Phys. Rev. C **80**, 014909 (2009).
[28] P. Braun-Munzinger, J. Stachel, J. P. Wessels, and N. Xu, Phys. Lett. B **344**, 43 (1995).
[29] R. C. Hwa and C. B. Yang, Phys. Rev. C **70**, 024905 (2004).
[30] V. Greco, C. M. Ko, and I. Vitev, Phys. Rev. C **71**, 041901 (2005).
[31] J. Zimányi, T. S. Biró, T. Csörgő, and P. Lévai, Phys. Lett. B **472**, 243 (2000).
[32] J. Song and F. L. Shao, Phys. Rev. C **88**, 027901 (2013).
[33] V. V. Anisovich and V. M. Shekhter, Nucl. Phys. B **55**, 455 (1973).
[34] F. L. Shao, Q. B. Xie, and Q. Wang, Phys. Rev. C **71**, 044903 (2005).
[35] B. Abelev *et al.* (ALICE Collaboration), Phys. Rev. Lett. **109**, 252301 (2012).
[36] K. A. Olive *et al.* (Particle Data Group), Chin. Phys. C **38**, 090001 (2014).
[37] B. Abelev *et al.* (ALICE Collaboration), Phys. Lett. B **718**, 279 (2012).
[38] P. V. Chliapnikov and V. A. Uvarov, Phys. Lett. B **240**, 519 (1990).
[39] A. Andronic, P. Braun-Munzinger, K. Redlich, and J. Stachel, arXiv:0707.4075.
[40] K. Aamodt *et al.* (ALICE Collaboration), Phys. Rev. Lett. **106**, 032301 (2011).
[41] T. Yao, Ph.D. thesis, Shandong University, 2009.
[42] K. Aamodt *et al.* (ALICE Collaboration), Phys. Lett. B **696**, 30 (2011).
[43] B. Abelev *et al.* (ALICE Collaboration), Phys. Rev. Lett. **111**, 222301 (2013).
[44] B. Abelev *et al.* (ALICE Collaboration), Phys. Lett. B **728**, 216 (2014).
[45] B. Abelev *et al.* (ALICE Collaboration), arXiv:1404.0495.
[46] A. Andronic, P. Braun-Munzinger, K. Redlich, and J. Stachel, Phys. Lett. B **571**, 36 (2003).
[47] R. C. Hwa and C. B. Yang, Phys. Rev. C **75**, 054904 (2007).
[48] L. W. Chen and C. M. Ko, Phys. Rev. C **73**, 044903 (2006).
[49] Y. F. Wang, F. L. Shao, J. Song, D. M. Wei, and Q. B. Xie, Chin. Phys. C **32**, 976 (2008).
[50] K. Zhang, J. Song, and F. L. Shao, Phys. Rev. C **86**, 014906 (2012).
[51] R. J. Fries, B. Muller, C. Nonaka, and S. A. Bass, Phys. Rev. Lett. **90**, 202303 (2003); Phys. Rev. C **68**, 044902 (2003).
[52] V. Greco, C. M. Ko, and P. Lévai, Phys. Rev. C **68**, 034904 (2003); Phys. Rev. Lett. **90**, 202302 (2003).
[53] T. S. Biró, P. Lévai, and J. Zimányi, Phys. Lett. B **347**, 6 (1995).
[54] Q. B. Xie and X. M. Liu, Phys. Rev. D **38**, 2169 (1988).
[55] F. L. Shao, T. Yao, and Q. B. Xie, Phys. Rev. C **75**, 034904 (2007).
[56] B. Abelev *et al.* (ALICE Collaboration), Phys. Lett. B **736**, 196 (2014).
[57] B. I. Abelev *et al.* (STAR Collaboration), Phys. Rev. Lett. **97**, 152301 (2006).
[58] A. M. Adare, M. P. McCumber, J. L. Nagle, and P. Romatschke, Phys. Rev. C **90**, 024911 (2014).
[59] S. S. Cao, G. Y. Qin, and S. A. Bass, Phys. Rev. C **88**, 044907 (2013).
[60] H. van Hees and R. Rapp, Phys. Rev. C **71**, 034907 (2005).
[61] G. M. Innocenti (for the ALICE Collaboration), Nucl. Phys. A **904-905**, 433c (2013).
[62] V. Topor Pop, M. Gyulassy, J. Barrette, C. Gale, and M. Petrovici, arXiv:1306.0885.